Electrochimica Acta 199 (2016) 133–141

Contents lists available at ScienceDirect

Electrochimica Acta

journal homepage: www.elsevier.com/locate/electacta

Label-free electrochemical multi-sites recognition of G-rich DNA using multi-walled carbon nanotubes–supported molecularly imprinted polymer with guanine sites of DNA

Min You[a], Shuai Yang[a], Fang Jiao[a], Li-zhu Yang[b], Fan Zhang[a,*], Pin-Gang He[a,*]

[a] School of Chemistry and Molecular Engineering, East China Normal University, 500 Dongchuan Road, Shanghai 200241, PR China
[b] School of Pharmaceutical Sciences, Wenzhou Medical University, Zhejiang 325035, PR China

ARTICLE INFO

Article history:
Received 2 December 2015
Received in revised form 24 March 2016
Accepted 25 March 2016
Available online 26 March 2016

Keywords:
label-free electrochemical strategy
MWCNTs-MIP
multi-sites recognition
guanine
G-rich DNA

ABSTRACT

A novel label-free electrochemical strategy was designed for multi-sites recognizing the guanine-rich DNA (G-rich DNA) with surface molecular imprinting polymer composite, in which the multi-walled carbon nanotubes (MWNCTs) were regarded as supporting material and the molecularly imprinted polymer (MIP) with guanine sites of DNA was applied as recognition element. Firstly, the vinyl groups were grafted onto the surface of carboxylic acid-functionalized MWNCTs (MWCNTs-COOH) through chemical modification. Then, the composite of MWCNTs-MIP was fabricated by the selective copolymerization of methacrylic acid, ethylene glycol dimethacrylate and guanine on the vinyl group-functionalized MWNTs surface. MWCNTs-MIP was characterized by different techniques, including Fourier transform infrared (FTIR) spectroscopy, scanning electronic microscopy (SEM), cyclic voltammogram (CV) and electrochemical impedance spectroscopy (EIS), showing that the MWCNTs-MIP composite was successfully prepared. Under the optimized conditions, the imprinting factor was nearly 5.68 according to the comparative slopes obtained on MWCNT-MIP and MWCNTs-non-imprinted polymer (MWCNTs-NIP), indicating that MWCNTs-MIP exhibited high selectivity for G-rich DNA. Moreover, the MWCNTs-MIP composite had a relatively wide linear range over G-rich DNA concentration of 0.05–1 μM and 5–30 μM with a detection limit of 7.52 nM (S/N = 3). Furthermore, the novel electrochemical strategy based on imprinted composite has very excellent performance in real samples of human serum and human urine.

1. Introduction

Deoxyribonucleic acid (DNA) is a kind of extremely important biological macromolecule, which plays a crucial role in the storage of genetic information and protein biosynthesis in living systems, and the detection of sequence-specific DNA is essential in many vital fields, such as rapid diagnosis of genetic diseases, gene expression analysis, biomedical screening and life sciences [1–3]. Recently, numerous techniques have been successfully applied to the analysis of sequence-specific DNA, including radio-assay, fluorescence, electrochemistry, gravimetric analysis etc. [4–7]. Electrochemical sensing technologies have many advantages, due to the high sensitivity, small dimensions, low cost, and compatibility with micro-manufacturing technology [8]. However, the label-free strategies are still challengeable and highly desirable for DNA recognition.

In recent years, surface molecular imprinting polymer (MIP) with the imprinted binding sites located at or very near the surface, has received a momentous amount of interest [9,10], which is usually fabricated on supporting materials, such as Au nanoparticles, carbon nanotubes, polyaniline nanofibers and metal-organic frameworks [11–14]. Compared to the traditional MIPs, surface MIP composite exhibits much better selectivity for recognizing biological macromolecules [15–17], due to their abundant three-dimensional cavities with specific shapes, sizes and functional groups [12,14]. However, most of published work related to surface MIP directly adopted biological macromolecules as templates, which limited the selectivity for target molecules, because of their unstable conformation and structures [18–21]. Therefore, it is a great challenge to develop highly selective detection method based on MIP for macromolecules.

In this work, a novel strategy for direct electrochemical multi-sites recognition of the G-rich DNA has been developed through

* Corresponding author. Tel.: +86 21 54340049; fax: +86 21 54340049.
E-mail addresses: fzhang@chem.ecnu.edu.cn (F. Zhang), pghe@chem.ecnu.edu.cn (P.-G. He).

http://dx.doi.org/10.1016/j.electacta.2016.03.151
0013-4686/

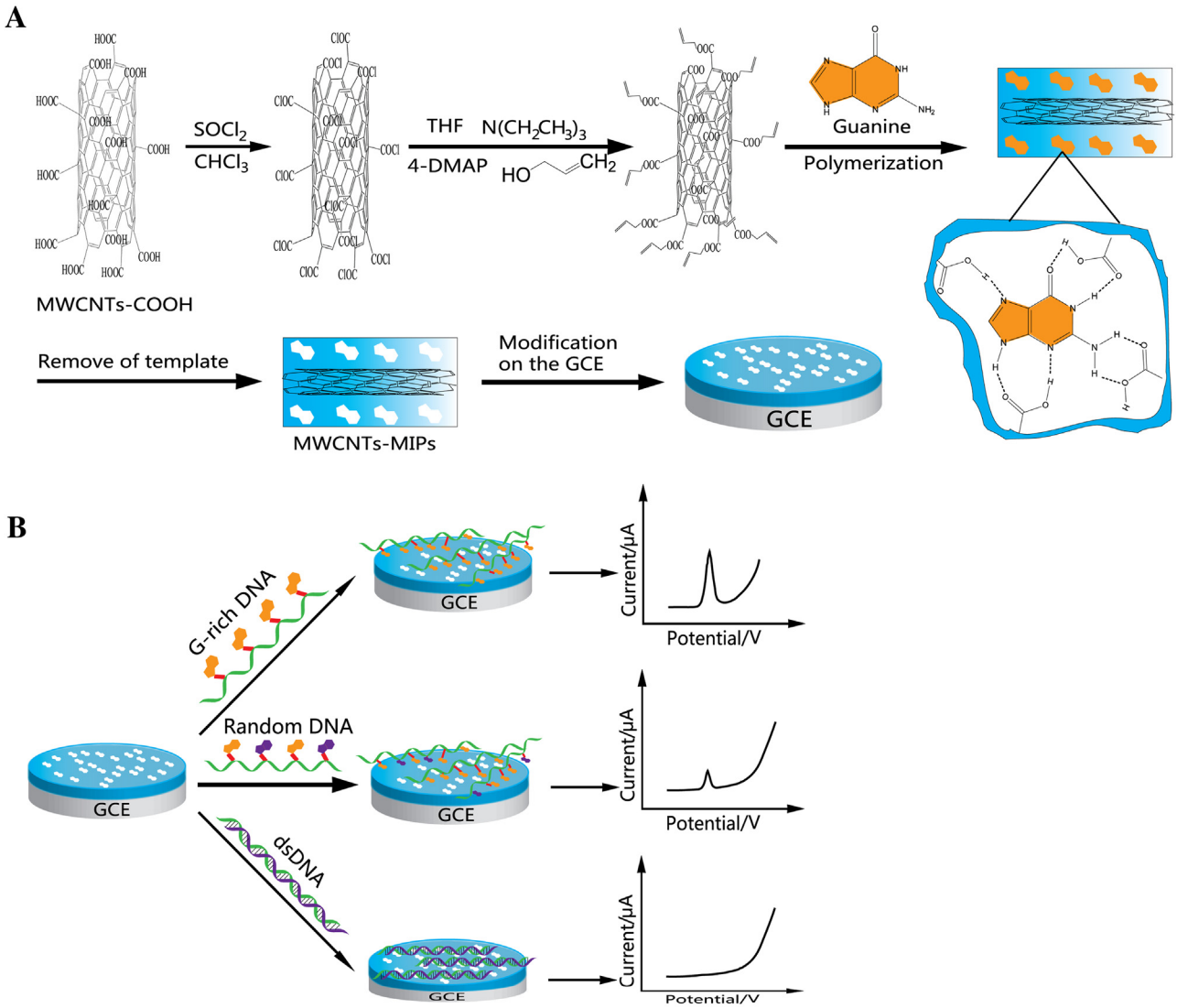

Scheme 1. (A) Schematic illustration of the preparation route for MWCNTs-MIP and the modified glassy carbon electrode. (B) The selective recognition principle of MWCNTs-MIP/GCE for the G-rich DNA before and after hybridization with its complementary sequence and the corresponding electrochemical responses.

the surface molecular imprinting technique, which has a high value on the investigation of DNA [22]. The schematic illustration of the assembly procedures for MIP composites and the electrochemical detection are indicated in Scheme 1. The surface MIP composite with molecular recognition capacity is developed with carboxylic acid-functionalized multiwalled carbon nanotubes as the supporting material, because of their attractive chemical, electronic and mechanical properties [23]. Guanine, the most redox-active nitrogenous base of DNA [24], is employed as template for the recognition of sequence-specific DNA, allowing the high selectivity of surface MIP composites via its strong multi-sites interaction with guanine nitrogenous base of G-rich DNA. Moreover, the direct electrochemical detection of G-rich DNA through surface MIP achieves electrochemical signals from the intrinsic electroactivity of DNA and avoids the complicated modification of redox mediators and the ineffective pre-immobilization process of probe DNA, which is applied to numerous DNA detection systems based on the hybridization between probe DNA and its complementary sequence [4–6]. To the best of our knowledge, this is the first report of MIP with guanine recognition sites of DNA for high sensitive and label-free DNA electrochemical sensing.

2. Experimental

2.1. Reagents

Carboxylic acid-functionalized multiwalled carbon nanotubes (MWCNTs-COOH) were obtained from Nanjing XFNANO Materials Tech Co. Ltd. (Nanjing, China). Methacrylic acid (MAA), methacrylamide (MAC), N, N′-methylenebis(acrylamide) (MBA), (4-dimethylamine) pyridine (4-DMAP), allyl alcohol and azobisisobutyronitrile (AIBN) were purchased from Sinopharm Chemical Reagent Co. Ltd (Shanghai, China). Guanine (G), ethylene glycol dimethacrylate (EGDMA), (4-dimethylamine) pyridine (4-DMAP), 1-vinylimidazole (1-VIM) and 4-vinylpyridine (4-VPY) were purchased from Sigma-Aldrich Chemical Co. (USA). 2′-Deoxyguanosine (2-DG), 2′-deoxyguanosine-5′-monophosphate (dGMP) and all the DNA sequences (Table 1) were obtained from Sangon Biotechology Inc. (Shanghai, China) with HPLC purification. MAA was distilled under reduced pressure to remove the polymerization inhibitor. AIBN was recrystallized from methanol before use. Human blood serum samples were collected from a local pathology laboratory and stored at 4 °C. 0.1 M phosphate buffer solution (PBS, pH = 7.4) prepared with double-distilled water was employed as

Table 1
DNA sequences.

Name	Sequence (5′ to 3′)	Name	Sequence (5‘ to 3')
$[G_6TG_6]$	GGG GGG T GGG GGG	$[G_3T]_4$	GGG TGG GTG GGT GGG T
$[G_2T]_6$	GGT GGT GGT GGT GGT GGT	$[G_3T]_5$	GGG TGG GTG GGT GGG TGG GT
$[G_4T]_3$	GGG GTG GGG TGG GGT	Random 1	GGT TGG TGT GGT TGG
$[G_3T]_3$ $[G_3]$	GGG TGG GTG GGT GGG	Random 2	AT GGA CAT GGC GGA
$T[G_3T]_4$	T GGG TGG GTG GGT GGG T	Random 3	TCT TTG GGA CCA CTG TCG
$TT[G_3T]_4T$	TT GGG TGG GTG GGT GGG TT	Random 4	ATC AGG GCT AAA GAG TGC AGA GTT ACT TAG
$TTT[G_3T]_4TT$	TTT GGG TGG GTG GGT GGG TTT	$c[G_3T]_4$-M_0	CCC ACC CAC CCA CCC A
$[G_3]_2$	GGG GGG	$c[G_3T]_4$-M_1	CCC ACC CCC CCA CCC A
$[G_3T]_2$	GGG TGG GT	$c[G_3T]_4$-M_2	CCC CCC CAC CCC CCC A
$[G_3T]_3$	GGG TGG GTG GGT	$c[G_3T]_4$-M_3	CCC CCC CCC CCC CCC A

the supporting electrolyte. All other solvents were of analytical reagent grade and used without further purification.

2.2. Apparatus

Fourier transform infrared (FTIR) spectroscopic measurements were performed on NEXUS 670 Fourier transform infrared spectrometer (Nicolet, USA). Surface morphological images were taken by a HITACHI S-4800 scanning electronic microscope (SEM, Hitachi Co. Ltd., Tokyo, Japan). Ultraviolet visible (UV–vis) absorption spectra were recorded by a U-3900H spectrophotometer (Hitachi High-Technologies Co., Japan). Electrochemical measurements were performed on a CHI 820b electrochemical workstation (CH Instruments Co., Shanghai, China) with a conventional three-electrode system comprising the modified or unmodified glass carbon electrode (3 mm in diameter) as working electrode, Ag/AgCl electrode with saturated KCl solution as reference electrode and platinum wire as auxiliary electrode in a 10 mL of glass cell containing electrolytic solution. All experiments were carried out at room temperature.

2.3. Preparation of MWCNTs-molecularly imprinted polymer (MWCNTs-MIP)

The synthesis of the vinyl group-functionalized MWNTs (MWCNTs-CH=CH_2) began with MWCNTs-COOH (0.4 g) [23], which was firstly suspended in the mixture containing 10 mL of sulfoxide chloride ($SOCl_2$) and 30 mL of chloroform at 60 °C for 24 h under reflux. The solid was washed by anhydrous tetrahydrofuran (THF) for several times to remove the excess $SOCl_2$ and dried under vacuum to obtain MWCNTs-COCl. Then, 0.2 g MWCNTs-COCl in 30 mL of anhydrous THF was mixed with 1.16 g allyl alcohol, 0.244 g 4-DMAP and 6.06 g trimethylamine, followed by stirring at 50 °C for 24 h. After washing with anhydrous THF and centrifugation, the obtained polymers was dried overnight in a vacuum desiccator, obtaining vinyl group-functionalized MWCNTs (MWCNTs-CH=CH_2).

MWCNTs-MIP with guanine sites was prepared by the bulk polymerization onto the surface of MWCNTs-CH=CH_2. In brief, 0.02 g MWCNTs-CH=CH_2 was added to the mixture solvent containing 30 mL of acetonitrile and 5 mL of toluene in a 250 mL round-bottom flask and purged with N_2 under magnetic stirring. 0.1 mmol guanine as template molecule and 0.5 mmol MAA as functional monomer dissolved by 5 mL of N, N′-dimethylformamide (DMF) were added to the reactor and mixed for 30 min. Then, 1.25 mmol EGDMA and 10 mg AIBN were also mixed, followed by the reaction at 70 °C for 12 h. The resulting composite was collected by centrifugation and washed thoroughly with ethanol to discard the reagents. In order to extract the template molecules, the composite was eluted by the mixture solvent of methanol and acetic acid (9:1, v/v) for several times until no guanine could be detected by UV–vis (at 244 nm and 274 nm) in the eluent. The obtained polymer was finally rinsed with ethanol to remove the remaining acetic acid and dried in the vacuum desiccator for 24 h before use. For comparison, MWCNTs-NIP was prepared by the same procedures, just without the template molecule in the polymerization process.

2.4. Preparation of MWCNTs-MIP modified electrode

Scheme 1A illustrated the preparation of MWCNTs-MIP and the formation of sensor. The bare GCE was polished with slurry alumina (0.05 μm) and washed thoroughly with double-distilled water and ethanol by the aid of ultrasonication. Then, 5.0 μL of MWCNTs-MIP suspension (1 mg/mL in DMF) was dropped on the cleaned GCE. After the solvent was evaporated at room temperature, the modified electrode was immersed in 0.1 M PBS for 10 min and dried in air. Thus, MWCNTs-MIP modified GCE (MWCNTs-MIP/GCE) was obtained. Also, MWCNTs-NIP/GCE was prepared in the similar process.

2.5. Electrochemical measurements

MWCNTs-MIP/GCE was incubated in 5.0 mL of DNA solution at different concentrations for 8 min and dried in air at room temperature, and then examined in 0.1 M PBS (pH = 7.4) by differential pulse voltammogram in the range of 0.7–1.2 V. The pulse amplitude, pulse period and pulse width of DPV were set at 50 mV, 0.1 s and 50 ms, respectively. After the measurements, the electrodes were rinsed with 5.0 mL PBS to remove DNA and dried in air for reuse. All experiments were carried out at room temperature (25 ± 1 °C). The current responses of DNA at MWCNTs-NIP/GCE in 0.1 M PBS (pH = 7.4) was employed as control. Similarly, voltammetric runs were also obtained on MWCNTs-NIP/GCE under identical operating conditions as mentioned above.

3. Results and Discussion

3.1. Characterization of MWCNTs-MIP

To ascertain the presence of guanine sites in the imprinted materials, MWCNTs-COOH, MWCNTs-NIP, MWCNTs-MIP and MWCNTs-MIP-guanine were characterized by FTIR, as shown in Fig. 1. The obvious infrared absorbance peaks at 3564 cm^{-1} and 1796 cm^{-1} were the features of carboxyl group in MWCNTs-COOH (Fig. 1, curve a). While, the characteristic peaks of MWCNTs-MIP-guanine were located at 3445 cm^{-1}, 3348 cm^{-1} and 1158 cm^{-1}, which were attributed to the stretching vibration and bending vibration of NH_2 in guanine, respectively (Fig. 1, curve c) [25,26]. Moreover, the main absorption bands of MWCNTs-MIP-guanine situating around 1731 cm^{-1}, 1634 cm^{-1}, 1390 $cm^{-1}$and 1257 cm^{-1} were assigned to C=O stretching and N—H bending vibration of acylamino, C—N stretching vibration, and the coupling effect between C—N and N—H [27–29], showing that guanine was

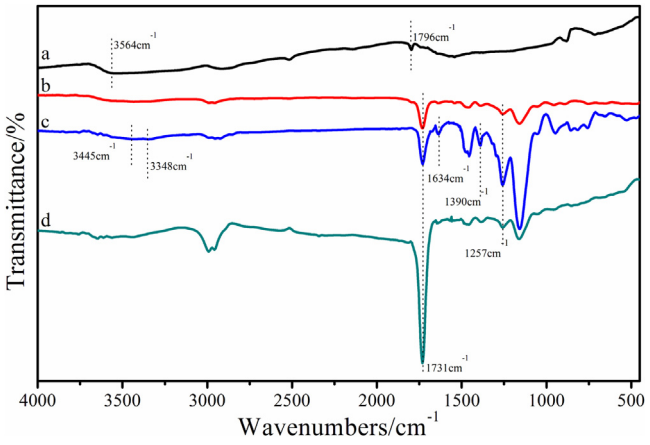

Fig. 1. FTIR spectra of (a) MWCNTs-COOH, (b) MWCNTs-NIP, (c) MWCNTs-MIP-guanine and (d) MWCNTs-MIP.

entirely embedded in the imprinted composites through the interaction between the template and monomer. After removal of guanine, the infrared absorbance peaks at 1634 cm^{-1} and 1390 cm^{-1} of amino group on guanine were disappeared, illustrating that guanine were successfully extracted from the imprinted material MWCNTs-MIP (Fig. 1, curve d), and the major bands of MWCNTs-NIP composites showed similar locations compared with MWCNTs-MIP (Fig. 1, curve b). The results indicated that guanine had been removed from MWCNTs-MIP.

The morphological structures of MWCNTs-COOH and MWCNTs-MIP were further characterized by SEM. The average thickness of the wall and length of MWCNTs-COOH were ~20 nm and ~2 μm, respectively (Fig. 2A). After polymerization, the side wall was indistinct (Fig. 2B) and the outer polymers shell with a diameter of ~50 nm were obtained, and MWCNTs-COOH was densely covered by MIP. In conclusion, the polymer of MIP was grafted to the surface of MWCNTs-COO-CH_2-CH=CH_2.

3.2. Electrochemical characterization of the modified electrodes

The electrochemical behaviours of bare GCE and the electrodes modified by MWCNTs-MIP, MWCNTs-NIP and MWCNTs-COOH were investigated by cyclic voltammogram (CV) and electrochemical impedance spectroscopy (EIS). Fig. 3A showed the CVs of K_3[Fe$(CN)_6$] at different electrodes with a scan rate of 100 mV/s. Clearly, a reversible peaks appeared at the bare GCE with a peak potential difference of 75 mV and a peak current ratio of about 1:1 (Fig. 3A, curve a). When the electrode was coated with MWCNTs-COOH, the redox peak current increased (Fig. 3A, curve c), because MWCNTs-COOH could promote the electron transfer. With the modification of MWCNTs-NIP on GCE, an obvious decrease in redox peak current (Fig. 3A, curve b) was observed in comparison to that of MWCNTs-COOH modified GCE, because the outer polymers shell of MWCNTs-NIP could block the electron transfer and the composite was lack of the three-dimensional cavities to accelerate the diffusion of $[Fe(CN)_6]^{3-/4-}$ [30]. While, after the coating of MWCNTs-MIP on GCE, the redox peak current (Fig. 3A, curve d) increased significantly, indicating that after removal of template molecule–guanine, the cavities produced in the imprinted membrane could enhance the diffusion of $[Fe(CN)_6]^{3-/4-}$ through the membrane and promote the redox reaction of $[Fe(CN)_6]^{3-/4-}$ on the electrode surface. The EIS results in Fig. 3B and the CV results of ferrocene methanol (Fc-CH_2OH) in Fig. 3C were consistent with that of CVs of K_3[Fe$(CN)_6$], further demonstrating the successful fabrication of MWCNTs-MIP.

3.3. Optimization of experimental variables

3.3.1. Effect of the functional monomers and the templates on the affinity of MWCNTs-MIP for G-rich DNA

In order to obtain the most excellent recognition capability of MWCNTs-MIP for G-rich DNA ($[G_3T]_4$,Table 1) [31], the functional monomers used in its synthesis process were first optimized among MAA, MAC, MBA, 1-VIM and 4-VPY. Simultaneously, the binding efficiency of relevantly different NIP composites also were investigated as control. MAA and MAC were employed due to their analogous structure and functional groups, which could coordinate with guanine. 1-VIM and 4-VPY were used for their positive-charged groups, because of the electrostatic interaction between negative-charged G-rich DNA and MIP. MBA was tested because of the couple of acylamino groups for coordination. As shown in Fig. 4A, MIP material with MAA showed higher affinity for G-rich DNA, compared with the other monomers, which was ascribed to the cavities of the composites matching the carboxyl group and three-dimensional shape of guanine. Therefore, MAA was selected as the functional monomer.

The structure of template molecules could also affect the affinity of MWCNTs-MIP for $[G_3T]_4$, so guanine, 2′-deoxyguanosine (2-DG) and 2′-deoxyguanosine-5′-monophosphate (dGMP) with the analogous structure were utilized respectively to synthesis the composites [32,33]. Clearly, MWCNTs-MIP with these three template molecules all exhibited DPV responses (Fig. 4B), showing

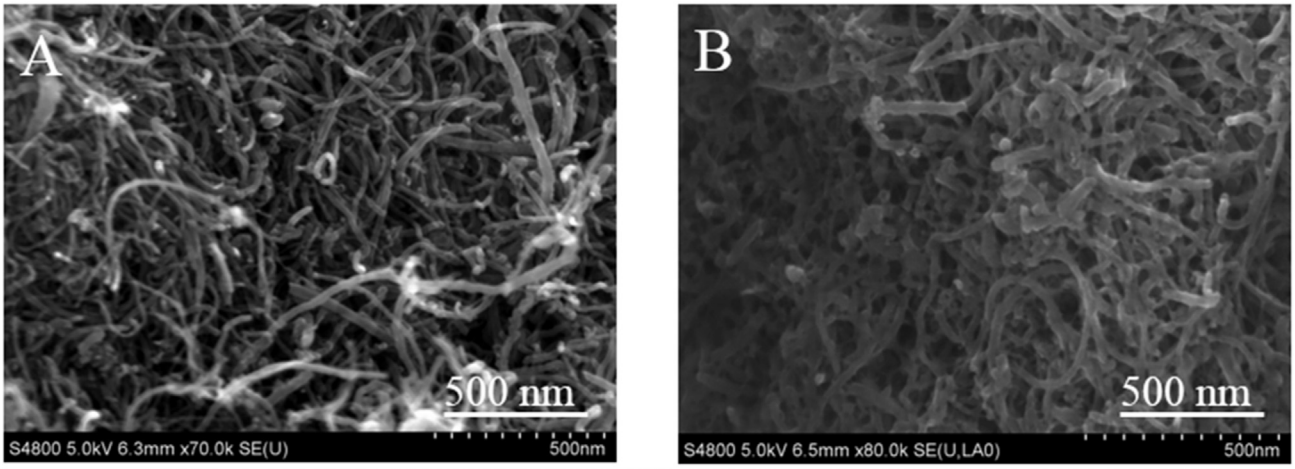

Fig. 2. SEM images of (A) MWCNTs-COOH and (B) MWCNTs-MIP.

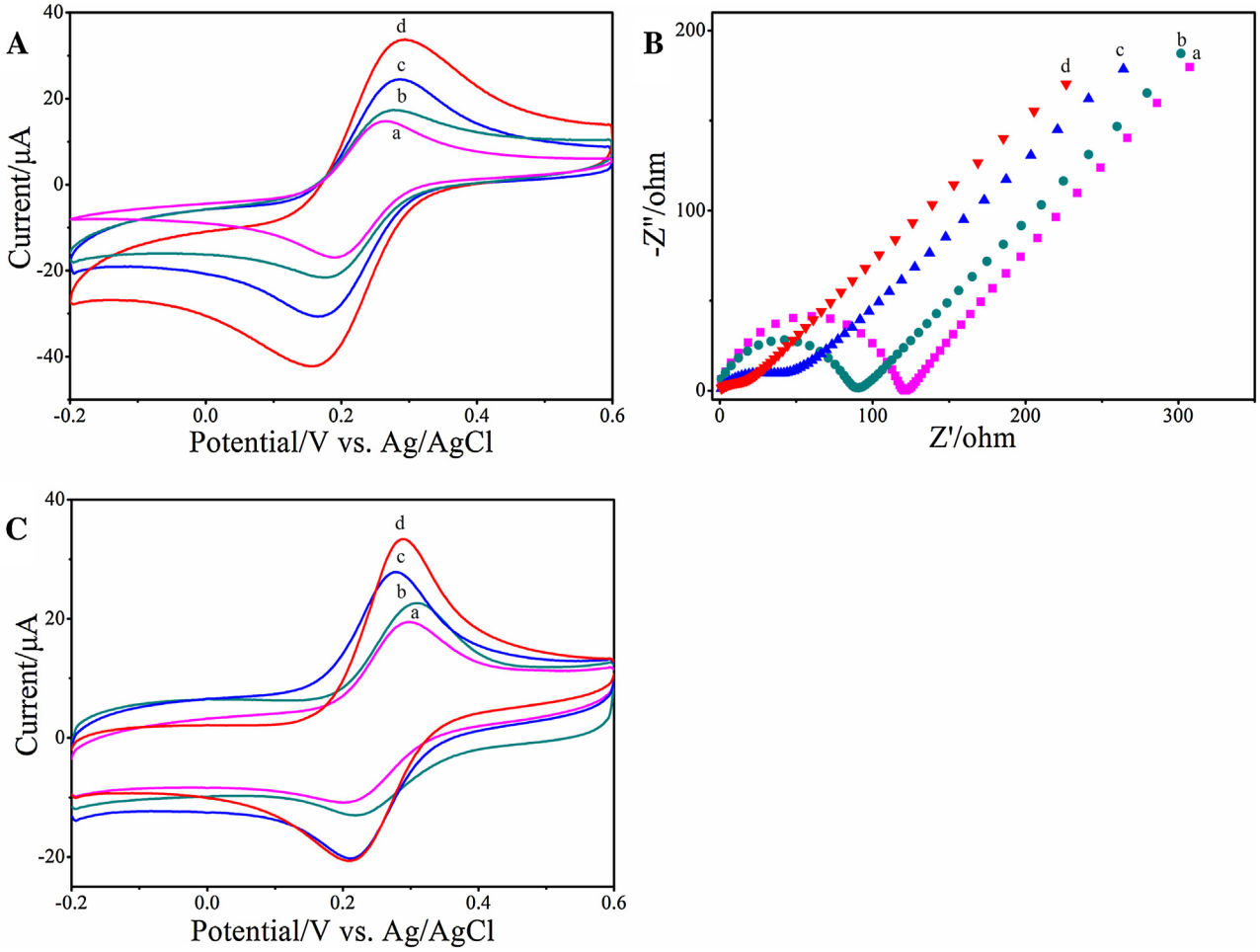

Fig. 3. (A) Cyclic voltammograms of 1 mM $K_3[Fe(CN)_6]$ in 0.1 M KCl at (a) bare GCE, (b) MWCNTs-NIP/GCE, (c) MWCNTs-COOH/GCE and (d) MWCNTs-MIP/GCE. (B) Electrochemical impedance spectra of 10 mM $K_3[Fe(CN)_6]/K_4[Fe(CN)_6]$ in 0.1 M KCl at (a) bare GCE, (b) MWCNTs-NIP/GCE, (c) MWCNTs-COOH/GCE and (d) MWCNTs-MIP/GCE. The frequency range is between 0.01 and 10^5 Hz. (C) Cyclic voltammograms of 1 mM Fc-CH_2OH in 0.1 M KCl at (a) bare GCE, (b) MWCNTs-NIP/GCE, (c) MWCNTs-COOH/GCE and (d) MWCNTs-MIP/GCE.

the presence of selective binding sites in the three composites. However, MWCNTs-MIP with guanine as the template presented the largest peak current, indicating its stronger binding capacity than the other two composites. The reason is that compared with the rigid structure of guanine, 2-DG and dGMP have mutable conformations [21], which decrease the ability of MWCNTs-MIP to selectively recognize G-rich DNA. Besides, the mainly exposed portions of ssDNA are nitrogenous bases, which also enhances the interactions between G-rich DNA and MWCNTs-MIP with guanine recognition sites. Hence, guanine was appropriated for the template of MWCNTs-MIP composite.

3.3.2. Effect of adsorption time and pH value of DNA incubation solution on the interaction between MWCNTs-MIP and G-rich DNA

The selective determination of G-rich DNA was realized through its adsorption on MWCNTs-MIP/GCE. Therefore, the adsorption time could affect the binding capability between MWCNTs-MIP and G-rich DNA. This effect was investigated by varying the

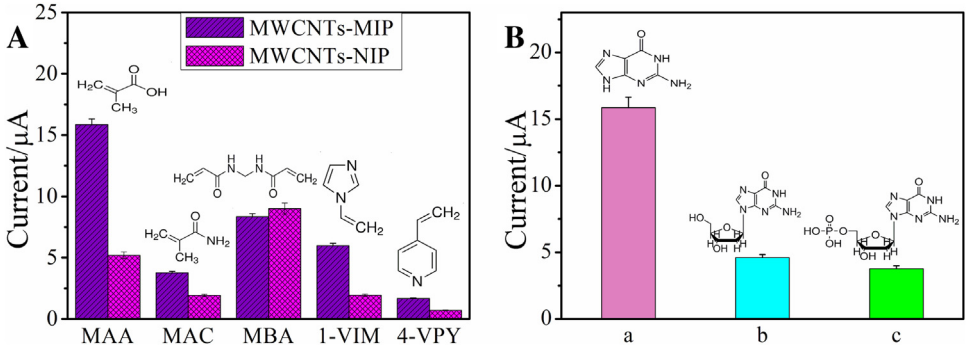

Fig. 4. (A) DPV responses of 5 μM $[G_3T]_4$ at MWCNTs-MIP/GCE and MWCNTs-NIP/GCE with different functional monomers. (B) DPV responses of 5 μM $[G_3T]_4$ at MWCNTs-MIP/GCE with different templates: (a) guanine, (b) 2-DG and (c) dGMP in PBS.

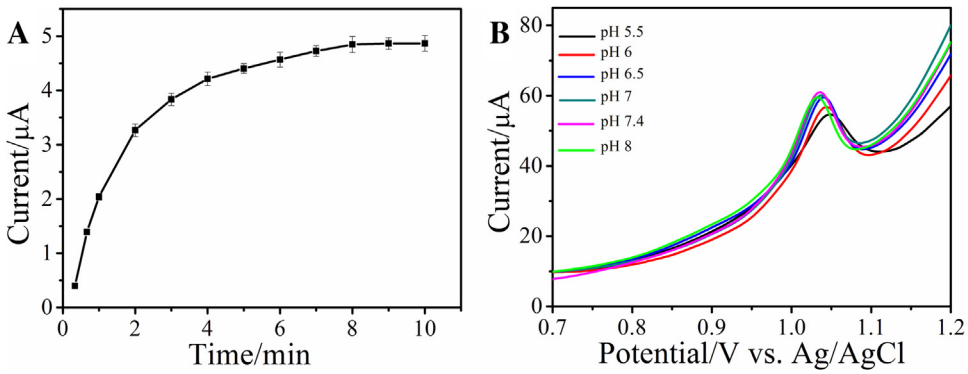

Fig. 5. (A) Current intensity of 1 μM $[G_3T]_4$ at MWCNTs-MIP/GCE with different adsorption time. (B) DPV responses of 10 μM $[G_3T]_4$ at MWCNTs-MIP/GCE with different pH values of incubation solution.

immersion time of MWCNTs-MIP/GCE into 1 μM $[G_3T]_4$ from 20 s to 10 min (Fig. 5A). Obviously, the adsorption of $[G_3T]_4$ to MWCNTs-MIP reached the equilibrium within 8 min, assisted by the surface-selective binding sites of MWCNTs-MIP. So, 8 min was chosen as the adsorption time of G-rich DNA.

The pH value of incubation solution for DNA binding with MWCNTs-MIP was also a very significant influence on the recognition selectivity for G-rich DNA. From Fig. 5B, it could be observed that the oxidation peak current continuously increased in the pH range of 5.5–7.4, maybe because more carboxylic acid groups in MWCNTs-MIP bound with $[G_3T]_4$. When the pH value reached 8, the declined current was obtained, due to the decreased amount of hydrogen bond between the MWCNTs-MIP composite and $[G_3T]_4$ in aqueous solution. Consequently, 0.1 M PBS solution with pH 7.4 was chosen as the most suitable incubation solution.

3.4. Selectivity of MWCNTs-MIP for G-rich DNA

With guanine as the template, DPV responses of MWCNTs-MIP/GCE, MWCNTs-NIP/GCE and MWCNTs-COOH/GCE were measured after incubation with 5 μM G-rich DNA–$[G_3T]_4$ for 8 min at a scan rate of 50 mV/s. As shown in Fig. 6A, a characteristic oxidation peak of $[G_3T]_4$ at ~1.02 V obtained from three modified electrodes could be observed. However, MWCNTs-NIP/GCE (Fig. 6A, curve c) presented the smaller current than MWCNTs-COOH/GCE (Fig. 6A, curve b), because the excellent electronic properties of MWCNTs-COOH accelerates the electron transfer between G-rich DNA and modified electrode. The current intensity of MWCNTs-NIP/GCE (Fig. 6A, curve c) was also smaller than that of MWCNTs-MIP/GCE, which could be explained that the MWCNTs-MIP has many three-dimensional cavities for binding G-rich DNA, while, MWCNTs-NIP could just adsorb a little of G-rich DNA. According to the oxidized peak currents of $[G_3T]_4$ recorded on MWCNTs-MIP/GCE and MWCNTs-NIP/GCE, indicating that the MWCNTs-MIP/GCE could recognize $[G_3T]_4$ selectively.

The binding selectivity of MWCNTs-MIP for G-rich DNA was investigated extensively with different DNA sequences (Table 1). Firstly, $[G_3T]_4$ and 4 random DNA sequences with different amount of guanine were selected to incubate with MWCNTs-MIP/GCE and MWCNTs-NIP/GCE in PBS (Fig. 6B). The DPV responses indicated

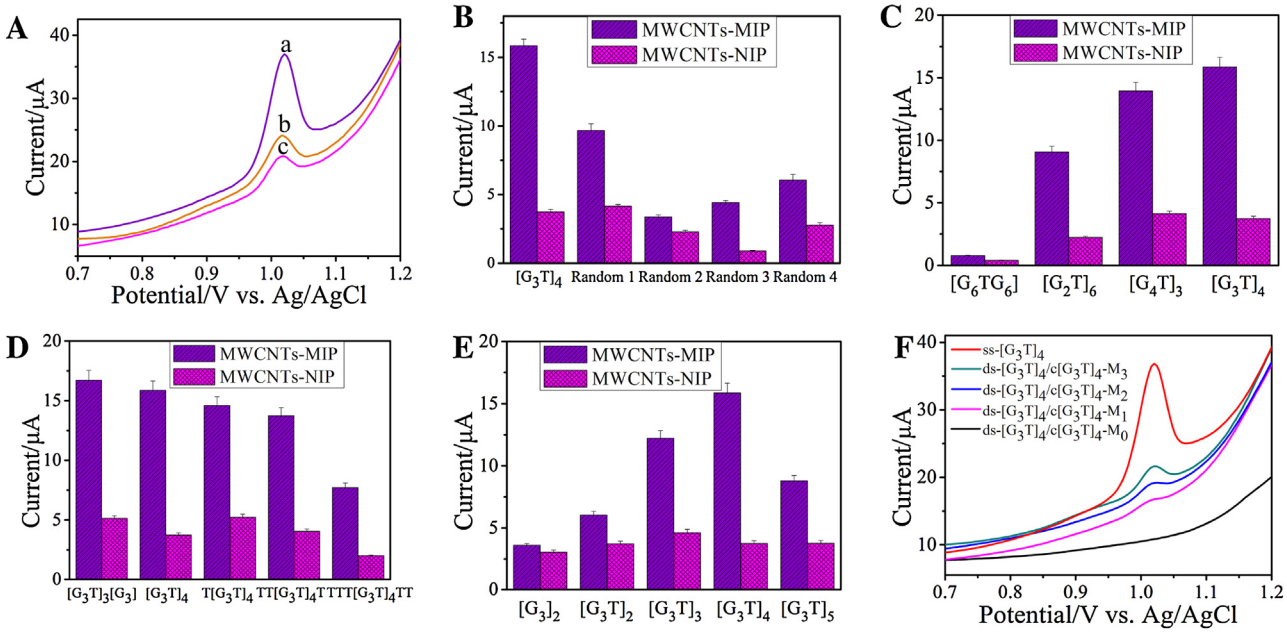

Fig. 6. (A) DPV responses of 5 μM $[G_3T]_4$ at (a) MWCNTs-MIP/GCE, (b) MWCNTs-COOH/GCE and (c) MWCNTs-NIP/GCE in PBS. (B) DPV responses of different random DNA sequences (5 μM) at MWCNTs-MIP/GCE and MWCNTs-NIP/GCE in PBS. (C) DPV responses of DNA sequences (5 μM) with different repeated segments at MWCNTs-MIP/GCE and MWCNTs-NIP/GCE in PBS. (D) DPV responses of DNA sequences (5 μM) with different terminal sequences at MWCNTs-MIP/GCE and MWCNTs-NIP/GCE in PBS. (E) DPV responses of 5 μM $[G_3]_2$, $[G_3T]_2$, $[G_3T]_3$, $[G_3T]_4$ and $[G_3T]_5$ at MWCNTs-MIP/GCE and MWCNTs-NIP/GCE. (F) DPV responses of $[G_3T]_4$ and its hybrids with 5 μM complementary DNA (c$[G_3T]_4$-M_0), single-base mismatched DNA (c$[G_3T]_4$-M_1), two-base mismatched DNA (c$[G_3T]_4$-M_2) and three-base mismatched DNA (c$[G_3T]_4$-M_3).

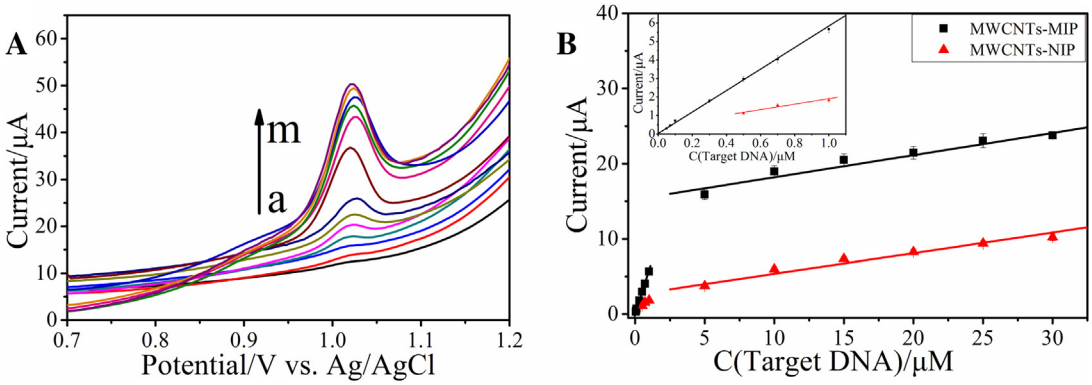

Fig. 7. (A) DPV responses of MWCNTs-MIP/GCE in PBS after incubation with $[G_3T]_4$ at different concentrations: (a) 0.05 μM, (b) 0.07 μM, (c) 0.1 μM, (d) 0.3 μM, (e) 0.5 μM, (f) 0.7 μM, (g) 1 μM, (h) 5 μM, (i) 10 μM, (j) 15 μM, (k) 20 μM, (l) 25 μM and (m) 30 μM for 8 min. (B) Calibration curve for the current intensity of MWCNTs-MIP/GCE and MWCNTs-NIP/GCE incubated with $[G_3T]_4$ as a function of its concentrations. Inset: the linear relationship between current response and a low concentration range.

MWCNTs-MIP had special recognition ability for the different DNA sequences, but the ability was different for the different amount of guanine in DNA, which could be attributed to the intrinsic electroactivity of guanine and the multi-sites interaction between guanine and MWCNTs-MIP. The current intensity of MWCNTs-MIP/GCE was larger than that of MWCNTs-NIP/GCE, showing that MWCNTs-MIP had stronger affinity to G-rich DNA due to the effect of guanine imprinting. Furthermore, $[G_3T]_4$ on MWCNTs-MIP/GCE presented the stronger current signal than the others, which was attributed to the synergistic effect of guanine [24] in the sequence GGGT in $[G_3T]_4$ and the imprinting cavities of MIP composites.

$[G_3T]_4$ and its analogs—$[G_6TG_6]$, $[G_2T]_6$, $[G_4T]_3$, with the same number of guanine were employed to verify the effect of the repeated sequence in DNA on the binding selectivity of MWCNTs-MIP for the G-rich DNA (Fig. 6C). It could be observed that the DNA sequence with the element of GGGT ($[G_3T]_4$) expressed the strongest electrochemical response, illustrating that the repeated sequence of GGGT was beneficial to the binding selectivity for G-rich DNA. The current response increased from GGT to GGGT, probably because base stacking could accelerate the electron transfer rate and enhances the reactivity of guanine multiplets [24]. On the other hand, the current response of GGGGGG or GGGGT decreased also, compared with GGGT. The possible reason is that the bulkiness of guanine multiplets in GGGGGG or GGGGT would enhance the interaction between DNA and decrease the amount of DNA bound with MWCNTs-MIP.

Fig. 6D showed that the current response of MWCNTs-MIP to $[G_3T]_4$ was higher than its analogs of $T[G_3T]_4$, $TT[G_3T]_4T$ and $TTT[G_3T]_4TT$. While, the response of MWCNTs-NIP was similar. The current intensity decreased with increasing the amount of terminal thymine ($[G_3T]_3[G_3]$, $[G_3T]_4$, $T[G_3T]_4$, $TT[G_3T]_4T$ and $TTT[G_3T]_4TT$), because the addition of terminal thymine increased the inhibition for the group of $[G_3T]_4$ to bind with the cavities of MWCNTs-MIP that reduced the affinity and selectivity between cavities of MWCNTs-MIP and $[G_3T]_4$. $[G_3T]_3[G_3]$ had stronger current intensity than $[G_3T]_4$, but its peak current ratio was lower than that of $[G_3T]_4$.

The quantity of repeated sequence GGGT was another important factor on the binding capacity of MWCNTs-MIP, which was evaluated by the determination of $[G_3T]_4$ and its analogs $[G_3]_2$, $[G_3T]_2$, $[G_3T]_3$ and $[G_3T]_5$ at MWCNTs-MIP/GCE and MWCNTs-NIP/GCE. As indicated in Fig. 6E, the responses of the G-rich DNA sequences at MWCNTs-MIP/GCE followed the order: $[G_3T]_4 > [G_3T]_3 > [G_3T]_5 > [G_3T]_2 > [G_3]_2$. $[G_3]_2$, $[G_3T]_2$ and $[G_3T]_3$ had the smaller signal than $[G_3T]_4$ and the intensity was enhanced with increasing the amount of GGGT, which increased the redox mediators and guanine binding sites in the G-rich DNA. The current response of $[G_3T]_5$ was still lower than that of $[G_3T]_4$, which could be ascribed to the declined amount of $[G_3T]_5$ captured by MWCNTs-MIP along with the molecular weight increasing of analyte. The results demonstrated that $[G_3T]_4$ had the selective interaction with MWCNTs-MIP.

Lastly, this work also exploited the selectivity of MWCNTs-MIP for ssDNA, dsDNA and partially hybridized dsDNA (Fig. 6F). Clearly, the DPV response of MWCNTs-MIP/GCE for dsDNA ($[G_3T]_4$ hybridized with its complementary DNA ($c[G_3T]_4$-M_0)) was hardly detected, because guanine was matched inside the dsDNA and no guanine was exposed to MWCNTs-MIP, leading to the disappearance of the characteristic oxidation peak. The current response of $[G_3T]_4$ hybridized with $c[G_3T]_4$-M_1, $c[G_3T]_4$-M_2 and $c[G_3T]_4$-M_3 increased successively, leading to the distinct discrimination. The results indicated that the MWCNTs-MIP could provide powerful selectivity for the recognition of ssDNA. To sum up, the above results showed that the MWCNTs-MIP had the most satisfactory recognition selectivity for G-rich DNA—$[G_3T]_4$.

3.5. Quantitative determination of G-rich DNA

The DPV responses of $[G_3T]_4$ under the optimized experimental conditions in Fig. 7 illustrated that the peak current was enhanced with increasing $[G_3T]_4$ concentration, and good linear relationship

Table 2
Comparison of different electrochemical methods for the determination of G-rich DNA.

Detection methods	Signal tag	Linear range (mol·L^{-1})	Detection limit (mol·L^{-1})	References
MWCNTs-PGE[a]	guanine	3.21×10^{-7}–6.42×10^{-6}	1.6×10^{-8}	[34]
stearic acid/CPE[b]	MB[c]	1.0×10^{-7}–1.0×10^{-4}	2.25×10^{-8}	[35]
ssDNA/GCE	MB	1.25×10^{-7}–6.75×10^{-7}	5.9×10^{-8}	[36]
MWCNTs-MIP/GCE	guanine	5.0×10^{-8}–3.0×10^{-5}	7.52×10^{-9}	This work

[a] PGE: pencil graphite electrode.
[b] CPE: carbon paste electrode.
[c] MB: methylene blue.

Table 3
Determination of sequence-specific DNA in real samples.

Name	[**]Detected (μM)	Added (μM)	Founded (μM)	Recovery (%)
Urine sample	Not found	0.5	0.44	88.04
		0.7	0.64	91.43
		1.0	0.93	93.47
[*]Serum sample (1%)	Not found	0.5	0.36	71.34
		0.7	0.56	79.80
		1.0	0.71	71.39

[*] Serum sample at high concentration is unsuitable to detecting the spiked G-rich DNA, and the human serum sample was deproteinized before use.
[**] Before spiking G-rich DNA in real samples, no electrochemical response was observed, indicating that no interferents in these real samples could be detected (below the detection limit of the proposed method).

between DPV response and DNA concentration was obtained in the range of 0.05–1 μM and 5–30 μM, respectively, with the detection limit of 7.52 nM (S/N = 3). The corresponding linear regression equations were i (μA) = 0.0356 + 5.86c (μM) (R = 0.9955) and i (μA) = 15.25 + 0.294c (μM) (R = 0.9791). In our viewpoint, this difference was caused by the adsorption mode of $[G_3T]_4$ and the relative amount of three-dimensional cavities on the surface of MWCNTs-MIP to $[G_3T]_4$. At lower concentration, selectivity adsorption of $[G_3T]_4$ was the predominant mode and the amount of three-dimensional cavities on the surface of MWCNTs-MIP was excessive, while, at higher concentration, mixed adsorption (specific and nonspecific adsorption) towards $[G_3T]_4$ played a dominant role and the cavity was insufficient, leading to the difference of linear responses. Furthermore, according to the comparative slopes in the range of 0.05–1 μM obtained on MWCNTs-MIP/GCE and MWCNTs-NIP/GCE, the imprinting factor with the value of 5.68 was calculated to evaluate the selectivity of MWCNTs-MIP toward $[G_3T]_4$, indicating further that MWCNTs-MIP could recognize G-rich DNA selectively.

The comparison of the MWCNTs-MIP/GCE with other electrochemical methods for DNA determination is listed in Table 2. The results demonstrate a relatively wide linear range and a low detection limit of the prepared MWCNTs-MIP composite, illustrating the advantages of MWCNTs-MIP with guanine sites of DNA.

In addition, the stability of MWCNTs-MIP was tested in 0.1 M PBS including 5 μM of $[G_3T]_4$. After stored for two weeks at room temperature, the response of MWCNTs-MIP/GCE retained 92.3% of the initial value; after one month-storage, the current intensity just declined by 13%. For the repeatability of MWCNTs-MIP/GCE, 12 electrodes were used for the repeated analyses of 5 μM $[G_3T]_4$ with a relative standard deviation (RSD) of 5.36% (n = 12). The results reflected the excellent stability and reproducibility of MWCNTs-MIP/GCE for G-rich DNA.

3.6. Real sample analysis

In order to examine the reliability of the proposed approach in practical applications, MWCNTs-MIP/GCE was applied to the detection of G-rich DNA in human urine and human serum (1%) samples (Table 3) [31]. The recovery tests of G-rich DNA ($[G_3T]_4$) at three concentrations (0.5, 0.7 and 1.0 μM) were performed through the standard addition method. The obtained recoveries of the human urine ranged from 88.04% to 93.47% and the human serum ranged from 71.34% to 79.80%, thereby validating the good recovery and practicability of MWCNTs-MIP for G-rich DNA in real samples.

4. Conclusions

In conclusion, a novel approach for label-free electrochemical detection of G-rich DNA was successfully demonstrated for the first time using MWCNTs-MIP with guanine recognition sites of DNA. The MIP composite was fabricated by bulk polymerization with the selective recognition portion of DNA–guanine as template, instead of DNA, extending the traditional mechanism of molecular imprinting technique that the imprinting of template was only applied to recognizing template molecule itself. The obtained MWCNTs-MIP showed high selectivity for recognizing G-rich DNA because of the abundant three-dimensional cavities of guanine sites in the composite. A wide linear range of 0.05–1 μM and 5–30 μM with a low detection limit of 7.52 nM (S/N = 3) for $[G_3T]_4$ determination was obtained under the optimized conditions with high stability and excellent reproducibility. Furthermore, the successful employment for the determination G-rich DNA in the human urine and human serum (1%) samples demonstrated the good practicability of this method. Our research can further promote the mechanisms research of sequence-specific DNA recognition with surface molecular imprinting technique.

Acknowledgements

This work was financially supported by the National Natural Science Foundation of China (Grant No. 21275054), Innovation Program of Shanghai Municipal Education Commission (Grant No. 13zz032) and Zhejiang Provincial Natural Science Foundation of China (Grant No. LQ12B05004).

References

[1] N.C. Seeman, DNA in a material world, Nature 421 (2003) 427–431.
[2] S. Husale, H.H. Persson, O. Sahin, DNA nanomechanics allows direct digital detection of complementary DNA and microRNA targets, Nature 462 (2009) 1075–1078.
[3] X. Wang, X. Zhang, P. He, Y. Fang, Sensitive detection of p53 tumor suppressor gene using an enzyme-based solid-state electrochemiluminescence sensing platform, Biosensors and Bioelectronics 26 (2011) 3608–3613.
[4] A. Sassolas, B.D. Leca-Bouvier, L.J. Blum, DNA biosensors and microarrays, Chemical Reviews 108 (2008) 109–139.
[5] W.-W. Zhao, J.-J. Xu, H.-Y. Chen, Photoelectrochemical DNA biosensors, Chemical Reviews 114 (2014) 7421–7441.
[6] E.G. Hvastkovs, D.A. Buttry, Recent advances in electrochemical DNA hybridization sensors, Analyst 135 (2010) 1817–1829.
[7] C. Fan, K.W. Plaxco, A.J. Heeger, Electrochemical interrogation of conformational changes as a reagentless method for the sequence-specific detection of DNA, Proceedings of the National Academy of Sciences 100 (2003) 9134–9137.
[8] H. Cai, X. Cao, Y. Jiang, P. He, Y. Fang, Carbon nanotube-enhanced electrochemical DNA biosensor for DNA hybridization detection, Analytical and Bioanalytical Chemistry 375 (2003) 287–293.
[9] K. Haupt, K. Mosbach, Molecularly imprinted polymers and their use in biomimetic sensors, Chemical Reviews 100 (2000) 2495–2504.
[10] K. Mosbach, The promise of molecular imprinting, Scientific American 295 (2006) 86–91.
[11] K. Qian, G. Fang, S. Wang, A novel core–shell molecularly imprinted polymer based on metal–organic frameworks as a matrix, Chemical Communications 47 (2011) 10118–10120.
[12] L. Ye, K. Mosbach, Molecular Imprinting: Synthetic Materials As Substitutes for Biological Antibodies and Receptors†, Chemistry of Materials 20 (2008) 859–868.
[13] C.S. Mahon, D.A. Fulton, Mimicking nature with synthetic macromolecules capable of recognition, Nature Chemistry 6 (2014) 665–672.

[14] R. Schirhagl, Bioapplications for Molecularly Imprinted Polymers, Analytical Chemistry 86 (2013) 250–261.
[15] S. Li, S. Cao, M.J. Whitcombe, S.A. Piletsky, Size matters: Challenges in imprinting macromolecules, Progress in Polymer Science 39 (2014) 145–163.
[16] Y. Lv, T. Tan, F. Svec, Molecular imprinting of proteins in polymers attached to the surface of nanomaterials for selective recognition of biomacromolecules, Biotechnology advances 31 (2013) 1172–1186.
[17] Z. Iskierko, P.S. Sharma, K. Bartold, A. Pietrzyk-Le, K. Noworyta, W. Kutner, Molecularly imprinted polymers for separating and sensing of macromolecular compounds and microorganisms, Biotechnology advances 34 (2016) 30–46.
[18] D.R. Kryscio, N.A. Peppas, Critical review and perspective of macromolecularly imprinted polymers, Acta Biomaterialia 8 (2012) 461–473.
[19] O. Slinchenko, A. Rachkov, H. Miyachi, M. Ogiso, N. Minoura, Imprinted polymer layer for recognizing double-stranded DNA, Biosensors and Bioelectronics 20 (2004) 1091–1097.
[20] M. Ogiso, N. Minoura, T. Shinbo, T. Shimizu, Detection of a specific DNA sequence by electrophoresis through a molecularly imprinted polymer, Biomaterials 27 (2006) 4177–4182.
[21] D.A. Spivak, K.J. Shea, Investigation into the scope and limitations of molecular imprinting with DNA molecules, Analytica Chimica Acta 435 (2001) 65–74.
[22] O. Doluca, J.M. Withers, V.V. Filichev, Molecular engineering of guanine-rich sequences: Z-DNA, DNA triplexes, and G-quadruplexes, Chemical Reviews 113 (2013) 3044–3083.
[23] X. Kan, Y. Zhao, Z. Geng, Z. Wang, J.-J. Zhu, Composites of multiwalled carbon nanotubes and molecularly imprinted polymers for dopamine recognition, The Journal of Physical Chemistry C 112 (2008) 4849–4854.
[24] F. Boussicault, M. Robert, Electron transfer in DNA and in DNA-related biological processes. Electrochemical insights, Chemical Reviews 108 (2008) 2622–2645.
[25] P. Turkewitsch, B. Wandelt, G.D. Darling, W.S. Powell, Fluorescent functional recognition sites through molecular imprinting. A polymer-based fluorescent chemosensor for aqueous cAMP, Analytical Chemistry 70 (1998) 2025–2030.
[26] S. Emir Diltemiz, A. Denizli, A. Ersöz, R. Say, Molecularly imprinted ligand-exchange recognition assay of DNA by SPR system using guanosine and guanine recognition sites of DNA, Sensors and Actuators B: Chemical 133 (2008) 484–488.
[27] M. Mathlouthi, A.M. Seuvre, J.L. Koenig, FT-IR and laser-Raman spectra of guanine and guanosine, Carbohydrate Research 146 (1986) 15–27.
[28] R. Santamaria, E. Charro, A. Zacarias, M. Castro, Vibrational spectra of nucleic acid bases and their Watson–Crick pair complexes, Journal of Computational Chemistry 20 (1999) 511–530.
[29] B.B. Prasad, R. Madhuri, M.P. Tiwari, P.S. Sharma, Imprinting molecular recognition sites on multiwalled carbon nanotubes surface for electrochemical detection of insulin in real samples, Electrochimica Acta 55 (2010) 9146–9156.
[30] A. Tiwari, S.R. Deshpande, H. Kobayashi, A.P. Turner, Detection of p53 gene point mutation using sequence-specific molecularly imprinted PoPD electrode, Biosensors and Bioelectronics 35 (2012) 224–229.
[31] M. Zhang, H.-N. Le, X.-Q. Jiang, B.-C. Yin, B.-C. Ye, Time-Resolved Probes Based on Guanine/Thymine-Rich DNA-Sensitized Luminescence of Terbium (III), Analytical Chemistry 85 (2013) 11665–11674.
[32] N. Sallacan, M. Zayats, T. Bourenko, A.B. Kharitonov, I. Willner, Imprinting of nucleotide and monosaccharide recognition sites in acrylamidephenylboronic acid-acrylamide copolymer membranes associated with electronic transducers, Analytical Chemistry 74 (2002) 702–712.
[33] S.E. Diltemiz, A. Denizli, A. Ersöz, R. Say, Molecularly imprinted ligand-exchange recognition assay of DNA by SPR system using guanosine and guanine recognition sites of DNA, Sensors and Actuators B: Chemical 133 (2008) 484–488.
[34] A. Erdem, P. Papakonstantinou, H. Murphy, Direct DNA hybridization at disposable graphite electrodes modified with carbon nanotubes, Analytical Chemistry 78 (2006) 6656–6659.
[35] Y. Ren, K. Jiao, G. Xu, W. Sun, H. Gao, An Electrochemical DNA Sensor Based on Electrodepositing Aluminum Ion Films on Stearic Acid-Modified Carbon Paste Electrode and Its Application for the Detection of Specific Sequences Related to Bar Gene and CP4 Epsps Gene, Electroanalysis 17 (2005) 2182–2189.
[36] X.-H. Lin, P. Wu, W. Chen, Y.-F. Zhang, X.-H. Xia, Electrochemical DNA biosensor for the detection of short DNA species of Chronic Myelogenous Leukemia by using methylene blue, Talanta 72 (2007) 468–471.